Crystalline Morphology and Dynamical Crystallization of Antibacterial β-Polypropylene Composite

Xin Chen, Kancheng Mai

Key Laboratory for Polymeric Composites and Functional Materials, the Ministry of Education, School of Chemistry and Chemical Engineering, Materials Science Institute, Sun Yat-Sen University, Guangzhou 510275, People's Republic of China

Received 13 December 2007; accepted 30 March 2008
DOI 10.1002/app.28452
Published online 12 September 2008 in Wiley InterScience (www.interscience.wiley.com).

ABSTRACT: The crystalline morphology and dynamical crystallization of antibacterial polypropylene composite and pure polypropylene were investigated via differential scanning calorimeter (DSC), wide angle X-ray diffraction (WAXD), and real-time hot-stage optical microscopy (OM). The results reveal that the crystalline morphology of antibacterial PP composites changes with variations of the crystallization conditions and compositions. The crystalline phase consists of both α-PP and β-PP crystals. The content of β-PP decreases with the increase in antibacterial agent content and cooling rate. With the addition of β-nucleating agent, the morphologies of all dynamically crystallized antibacterial PP composites show no obvious spherulitic morphology, and the decrease of crystal perfection and the increase of nucleation density of antibacterial PP composite system could be observed. With the increase of antibacterial agent content, the overall crystallization rates of the antibacterial PP composite increase dramatically, while the content of β-PP in all antibacterial PP composite decrease distinctly under given cooling conditions. These results can be explained by the interruptive effect of antibacterial agent on interactions of β-nucleating agent components and the obstructing effect of antibacterial agent on the mobility of PP chains in melts. © 2008 Wiley Periodicals, Inc. J Appl Polym Sci 110: 3401–3409, 2008

Key words: antibacterial; β-polypropylene; crystallization; morphology; composites

INTRODUCTION

Silver-filled polymers are well-known antibacterial materials by virtue of their ability to release the biocidal species, viz. Ag^+ ions in an aqueous environment.[1–5] The mechanism of inhibitory action of sliver ions on microbes is partially known. It is believed that DNA loses its replication ability and cellular proteins become inactivated upon Ag^+ encounter.[6] Besides this, silver ions attack some functional groups in proteins, causing its danaturation.[7] Thermoplastic composites produced from Ag^+ containing powder-filled polymers have been recognized as capable of releasing silver ions.[8] The antibacterial activity in such composite system is decided by the ability of the emerging composites to release silver ions in a pathogenic environment.[9] Further research had indicated the importance of morphological variations of antibacterial composite on determining its antibacterial activity.[8] However, systematic research about the influence of morphological variations on antibacterial properties has not yet been reported.

Correspondence to: K. Mai (cesmkc@mail.sysu.edu.cn).

Journal of Applied Polymer Science, Vol. 110, 3401–3409 (2008)

Isotactic polypropylene (PP) is well known to simultaneously crystallize into two crystalline forms, α and β phase.[10] The β phase has been reported to have higher ductility than α phase[11–15] with little loss of stiffness.[13,14] Therefore, the dependency of antibacterial activity on the morphological properties of composite can be obtained through a systematic research of the change of antibacterial properties of antibacterial polypropylene composite with variation of morphologies. To tackle the entire problem systematically, it is quite necessary to understand the crystalline morphology and the dynamically crystallization behavior of antibacterial polypropylene composites.

In this work, antibacterial β-polypropylene composites were *in situ* prepared, and measurements were conducted to study the structure, morphology, and nonisothermal crystallization behavior of antibacterial β-polypropylene composite under various antibacterial agent content and crystallization conditions.

EXPERIMENTAL

Materials

The grade of polypropylene used in this study was K8303, supplied by Sinopec Beijing Yanshan Petrochemical (PRC), with 17.8 mol percent (mol %) of

TABLE I
Composition of Pure PP and Antibacterial PP Composites

Sample	Content of polypropylene (phr)	Content of antibacterial agent (phr)	Content of β-nucleating agent (phr)
PP	100	0	0
PP 0	100	0	1
PP 1	100	1	1
PP 2	100	2	1
PP 3	100	3	1
PP 4	100	4	1

ethylene and a melt flow rate (measured at 230°C and 2.16 kg) of 1.39 g/10 min. Antibacterial agent used in this study was SR-T-101 (density = 2.6 g/cm^3, particle size = 0.65 μm), purchased from SR-Business. SR-T-101 is a hybrid product between silver as an active substance and an inorganic ion-exchanger as a carrier. It is widely used as an inorganic antibacterial agent and has a wide range of spectrum against a lot of organisms. β-nucleating agent was *in situ* formed with $CaCO_3$ and fatty dibasic acid.

Sample preparation

According to the composition listed in Table I, pure PP and antibacterial β-PP samples were prepared by melt blending in internal mixer at the temperature of 190°C for 5 min. After that, the samples were removed from the mixer and cooled down to room temperature.

Differential scanning calorimetry

A TA Q10 differential scanning calorimeter (DSC) with nitrogen as purge gas was used to investigate the crystallization behavior of the pure PP and antibacterial β-PP. Pure indium and zincum were used as standard materials to calibrate both the temperature scale and the melting enthalpy before the samples were tested. The samples (about 5.0 mg) were heated at 210°C for 5 min to eliminate thermal history and then cooled down to 30°C at constant cooling rates of 10, 15, 20, 25, and 30°C/min, respectively.

The percentage of β-PP for a sample, ϕ_β, was determined by the relative crystallinity of α- and β-PP according to eq. (1) as reported in Ref. 16.

$$\varphi_\beta = \frac{X_\beta}{X_\alpha + X_\beta} \times 100\% \quad (1)$$

where X_α and X_β are the crystallinity of the α- and β phases, respectively, based on specific fusion heats of the samples.

Considering the coexistence of α- and β-PP crystals in the samples, the crystallinity of each phase has been calculated separately according to eq. (2).

$$X_i = \frac{\Delta H_i}{\Delta H_i^\theta} \times 100\% \quad (2)$$

where ΔH_i is the calibrated specific fusion heat of either α- or β-PP crystals, while ΔH_i^θ is the standard fusion heat of either α- or β-PP crystals, which is 178 J/g for α-phase and 170 J/g for β-phase.[17]

The DSC curves of some samples exhibited melting peaks of both α- and β-phase. The specific fusion heats for α- and β-phase were determined according to the following calibration method. The total fusion heat, ΔH, was integrated from 90 to 180°C on the DSC thermogram. A vertical line was drawn through the minimum between the melting peaks of α- and β-phase, and the total fusion heat was divided into the fusion heat of β-phase, ΔH_β^*, and fusion heat of α-phase, ΔH_α^*. Because the less perfect α-phase melts before the maximum point during heating and gives rise to ΔH_β^*, the true value of fusion heat of β-phase, ΔH_β^*, has been approximated by the production of multiplying ΔH_β^* with a calibration factor A:[18]

$$\Delta H_\beta = A \times \Delta H_\beta^* \quad (3)$$

$$A = \left[1 - \frac{h_2}{h_1}\right]^{0.6} \quad (4)$$

$$\Delta H_\alpha = \Delta H - \Delta H_\beta \quad (5)$$

where h_1 and h_2 are the heights from the base line to the melting peak of β-phase and the minimum point between melting peaks of α- and β-phase, respectively.

Optical microscopy

For optical microscopy observation, a Leiz Orthoplan pol polarizing microscope, equipped with Linkam THMS600 heating and cooling stage, and CCD color camera were used in this study. The samples sandwiched between two microscope cover slips were first heated to 210°C for 5 min to erase its thermal history and then cooled to room temperature (about 30°C) at cooling rate of 10°C/min.

The crystallization processes were *in situ* observed, and the morphologies were recorded at constant time intervals. All images presented in this work were taken under the crossed-polarized condition. The precision of controlled heating and cooling stage is less than ±0.1°C.

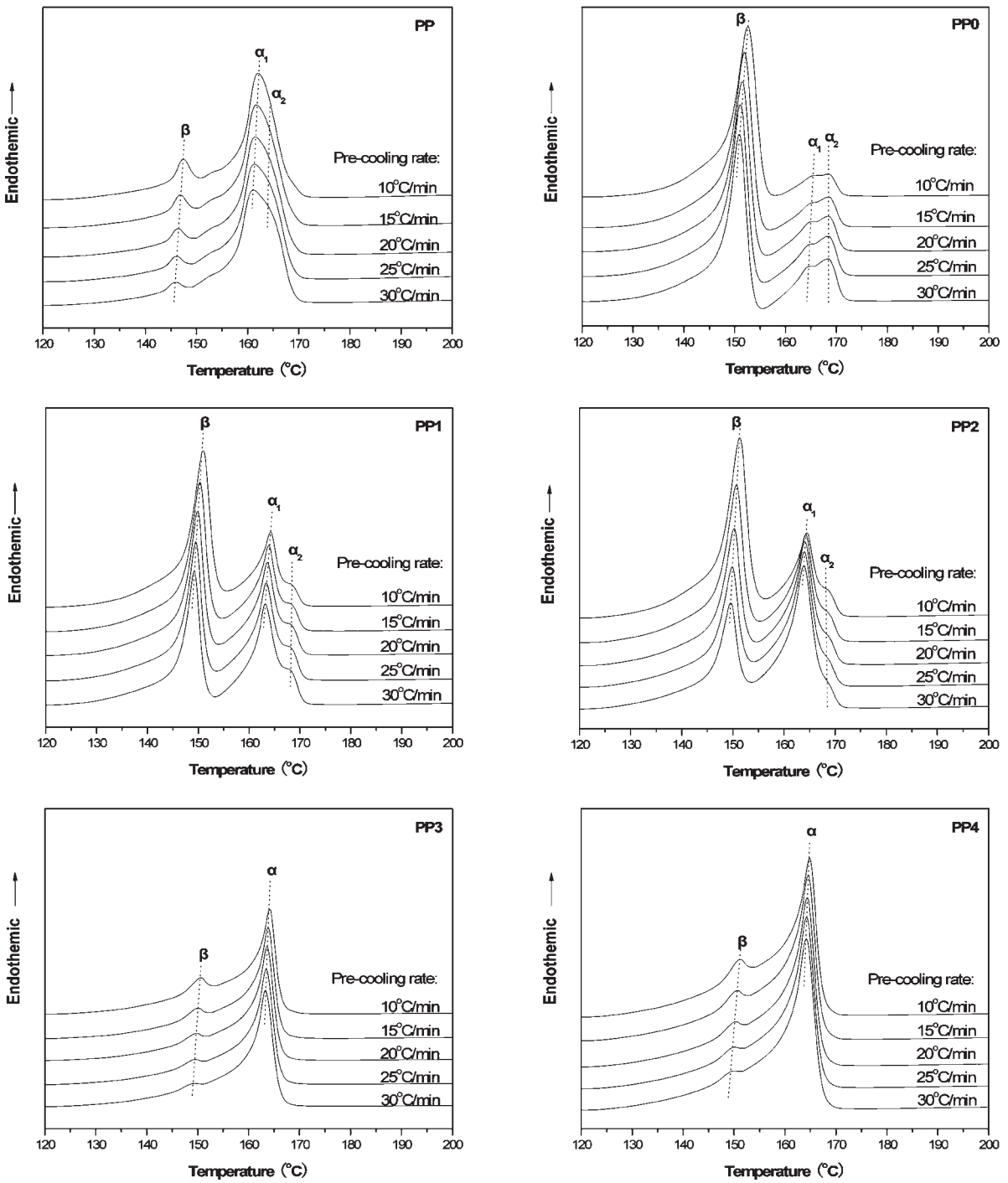

Figure 1 DSC melting curves of PP and various antibacterial PP composites prepared under different cooling rates (scanning rate: 10°C/min).

Wide angle X-ray diffraction

Wide-angle X-ray diffraction (WAXD) patterns were obtained using a Rigaku D/max-2200 VPC diffractometer with the Cu Kα radiation at room temperature. The operation condition of X-ray source was set at a voltage of 40 kV and a current of 30 mA in a range of $2\theta = 0$–50°.

RESULTS AND DISCUSSION

Melting behavior

The DSC melting curves of pure PP and antibacterial β-PP composites crystallized at various cooling rates are shown in Figure 1. Obviously, the melting curves of all specimens demonstrate at least two melting

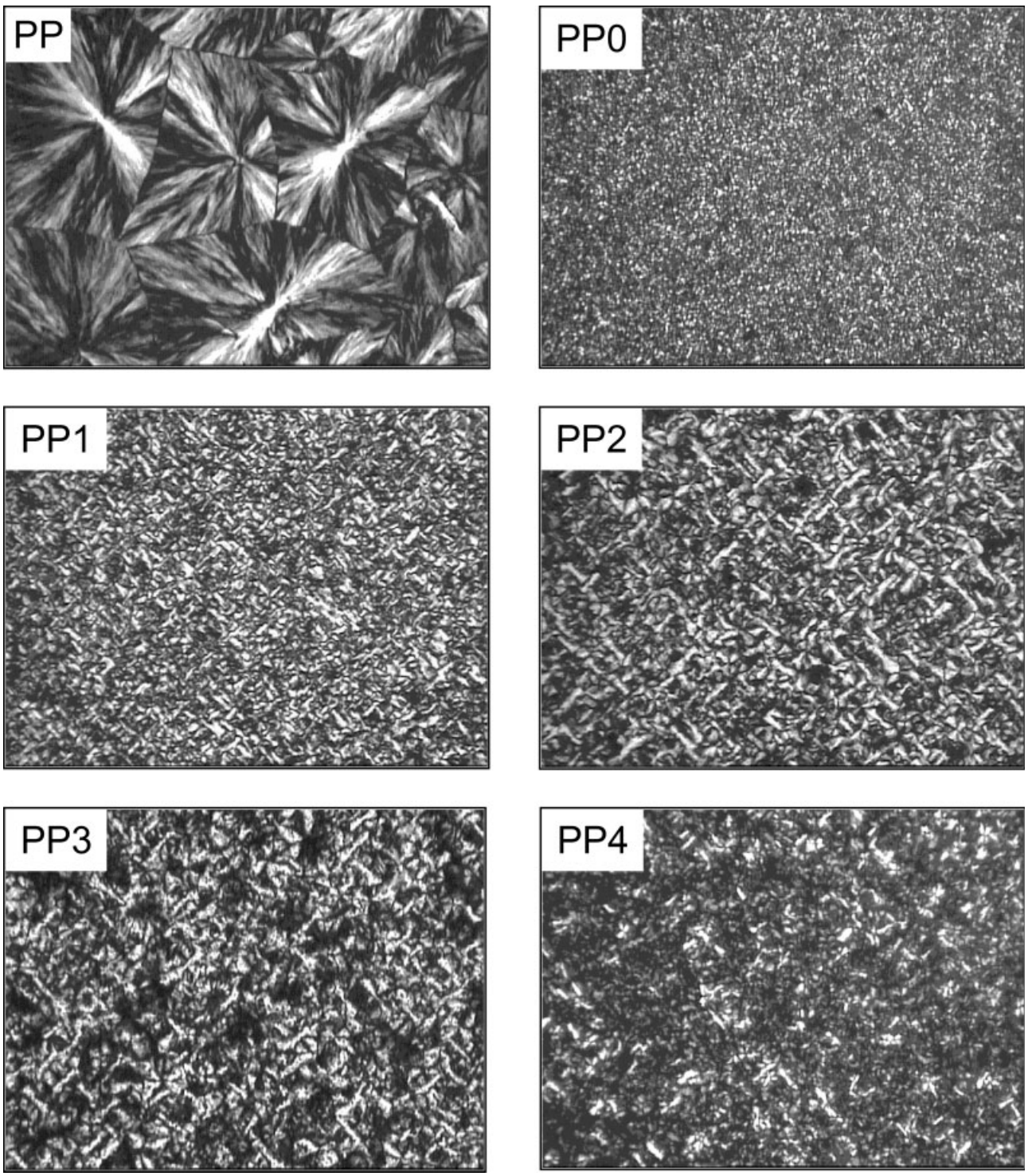

Figure 2 Optical morphologies of pure PP and antibacterial PP composites crystallized at cooling rate of 10°C/min.

peaks around 147 and 163°C. For PP, the double-melting peaks shift to lower temperature with the increase of cooling rates, and a shoulder peak appears around 147°C. For PP0 specimen, the peak around 147°C strengthens greatly while a third melting peak appears at about 167–170°C. With the increase in antibacterial agent content, peaks at about 144–148°C and 167–170°C seem to weaken while peaks at about 163–165°C strengthen. Moreover, for PP3 and PP4 samples, with antibacterial agent content of 3 and 4 phr, respectively, the third melting peak at about 167–170°C disappears and the peak at about 144–148°C turns into small shoulder peak under all sample preparation conditions.

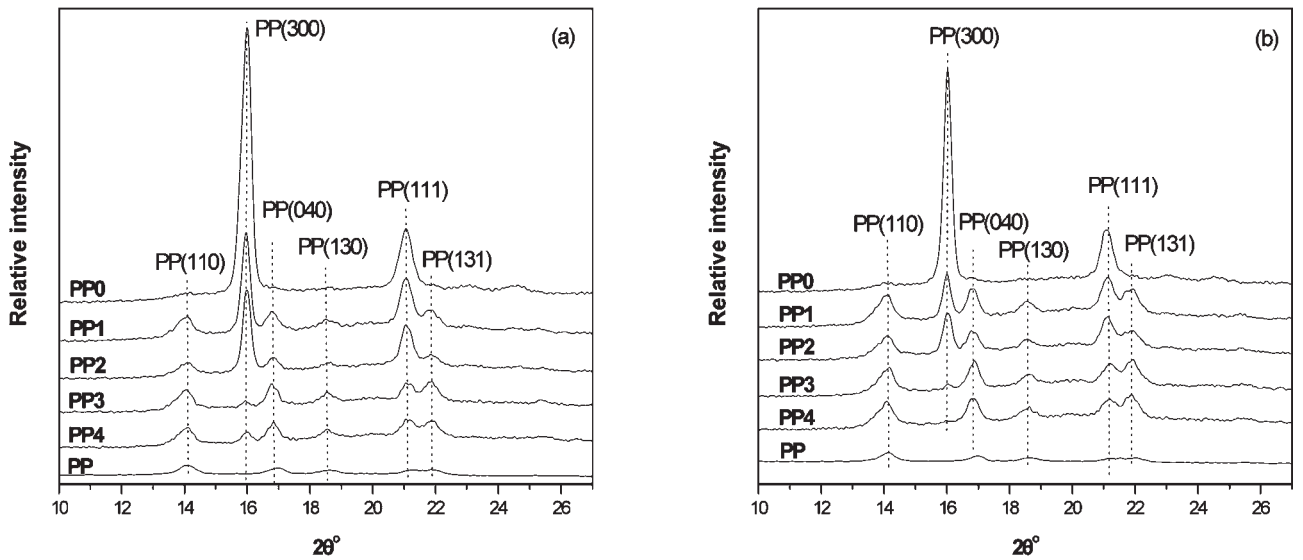

Figure 3 WAXD patterns of PP and antibacterial PP composites crystallized at different cooling rates: (a) 10°C/min and (b) 30°C/min.

It is documented that the multiple melting behavior of PP depends on the thermal conditions of crystallization by many researches.[19–22] Petracone et al. reported that the existing of less-ordered α_1 and more-ordered α_2 forms with a well-defined deposition of up and down helices in the unit cells could result in the double-melting peaks.[19–21] The existence of two phases, α_1 and α_2, for PP was further confirmed using SAX and DSC techniques.[22] Thus, in Figure 1, the double α-melting peaks of antibacterial PP composite indicate the existence of α-crystal with different structure. With the increase in cooling rate, α_2-crystal content increases gradually while decreases with the increase of antibacterial agent content. Therefore, it is suggested that α_2 crystals are mainly formed by secondary crystallization of incomplete crystals. It is worth noting that the DSC curve illustrates the existence of β-PP in pure PP at all cooling rates. This has, however, not been identified in the WAXD experiments. This is understandable that the DSC measurement concerns the supermolecular structure of the sample, while the WAXD reflects the overall crystalline structure of the sample. As a result, some crystalline structure of the minority crystalline phase could be covered up by the majority phase.

Crystalline morphology

Figure 2 shows the morphologies of various antibacterial PP composite as well as pure PP crystallized at a cooling rate of 10°C/min. It can be seen that the morphology of pure PP specimen crystallized from the melt is spherulitic. As for the morphology of the antibacterial PP composite, it depends strongly on composition. For PP0 specimen with the β-nucleating agent of 1 phr, it is very difficult to distinguish any spherulites. The number of crystals formed increased dramatically while their dimension decreased. When 1 phr of antibacterial agent was added, the size of crystals formed for the PP1 specimen becomes bigger, and the number of crystal begins to decrease. However, with the further increasing of antibacterial agent, the dimensions of the crystals formed become smaller and spherulitic crystals become identical gradually. Moreover, for specimens with antibacterial agent content higher than 3 phr, it can be seen that the crystal morphol-

TABLE II
Overall Crystallinity and β-PP Content in Pure PP and Antibacterial PP Composite Crystallized at Different Cooling Rate

Cooling rate (°C/min)	PP		PP0		PP1		PP2		PP3		PP4	
	X_c (%)	φ_β (%)	X_c (%)	φ_β (%)	X_c (%)	φ_β (%)	X_c (%)	φ_β (%)	X_c (%)	φ_β (%)	X_c (%)	φ_β (%)
10	35.59	14.04	40.32	87.65	42.12	63.53	41.70	64.88	41.66	13.35	46.50	10.36
15	35.42	10.69	41.91	83.67	41.59	58.68	41.13	54.79	40.89	8.46	46.20	7.40
20	35.33	8.68	42.71	79.33	41.15	55.28	40.94	47.06	40.74	6.35	45.96	5.02
25	35.32	7.12	44.14	76.80	40.99	53.02	40.79	41.09	40.59	4.28	45.67	2.97
30	35.66	5.62	44.65	74.47	40.80	50.24	40.63	36.23	40.50	2.50	45.29	1.38

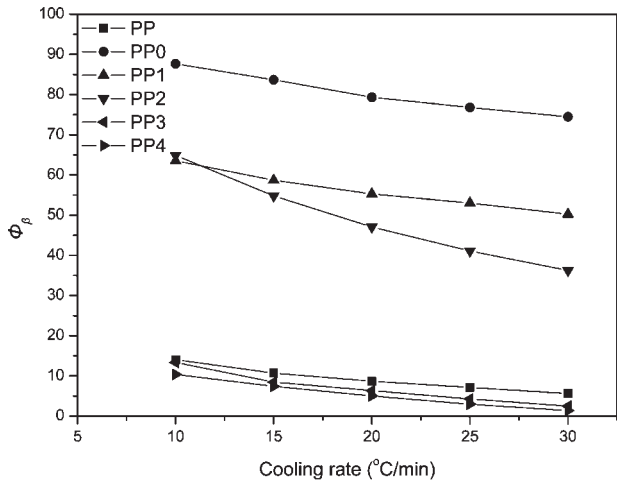

Figure 4 Dependence of β-PP content for pure PP and antibacterial PP composites on cooling rate.

ogy formed becomes more deficient. All these results clearly indicate that the existence of β-nucleating agent and antibacterial agent has influenced the crystallization morphologies of PP. They further imply that at high content of antibacterial agent, PP prefers to crystallize with antibacterial agent as the nuclei rather than with β-nucleating agent.

Crystal modification

To find out the crystalline structure of the antibacterial β-PP, WAXD was performed. Figure 3 shows the WAXD spectra of the specimens crystallized at cooling rate of 10 and 30°C/min, respectively. It can be seen from Figure 3(a) that all the most intense WAXD reflections at 2θ angles of 14.0°, 16.8°, 18.6°, 21.2°, and 21.9°, corresponding to the (110), (040), (130), (111), and (131) lattice planes of the most common α-monoclinic modification have appeared in the X-ray diffraction spectra of every sample. This clearly indicates that in all cases both pure PP and antibacterial PP composite crystals grow in monoclinic α-modification. For antibacterial PP composite, another peak appears at 2θ of 16.0°, which can be accounted for by the (300) lattice planes of the hexagonal β-modification.[23,24] There may be also the characteristic (301) β-modification reflection at 21.2°, which overlaps with the (111) lattice plane reflection of α-modification. The appearance of (300) β-modification indicates the existence of β-modification in the antibacterial PP composite specimens crystallized at cooling rates of 10 and 30°C/min. Moreover, the decrease in intensity of the (300) lattice plane reflection indicates that the content of β-modification decreases with the increase of antibacterial agent content in antibacterial PP composites and the increase of the cooling rate. This is in good accordance with the results of DSC measurement.

The total crystallinity and the β-modification content of the studied samples obtained from DSC data are listed in Table II. It can be clearly seen that the total crystallinity of pure PP changed slightly and antibacterial PP composites decreased generally with the increase of the cooling rate while that of β-PP with no antibacterial agent (PP0) increased under the same condition. At the same time, the β-PP content of all specimens, as plotted in Figure 4, decreases with the increase in cooling rate. Furthermore, the increase of antibacterial agent content in antibacterial PP composite results in the increase of the total crystallinity and the decrease of the β-PP content. This implies that the existence of antibacterial agent particles facilitates the crystallization of the whole antibacterial PP composite system, whereas they might go against the formation of β-PP crystals.

It was well reported that the monoclinic α-PP, the thermodynamically stable crystalline form, can be easily generated by melt crystallization. The nucleation of metastable β-form occurs much more rarely in bulk crystallization than that of the predominant α-modification. Nevertheless, both α- and β-PP crystals could coexist under several crystallization conditions, and the proportion of these two phases depends strongly on the thermal conditions and the way of nucleation.[10,23–35] It was suggested that the formation of β-PP supermolecular structure can be promoted from the sheared polymer melts in a certain temperature range.[34–39] More recently, it is suggested by the authors[40,41] that the orientation status of the PP chains in melting state plays a leading role in generating β-PP. At the present case, taking the fact into consideration that β-PP has been generated in antibacterial PP composite when $CaCO_3$ and fatty dibasic acid were added, the formation of β-PP in

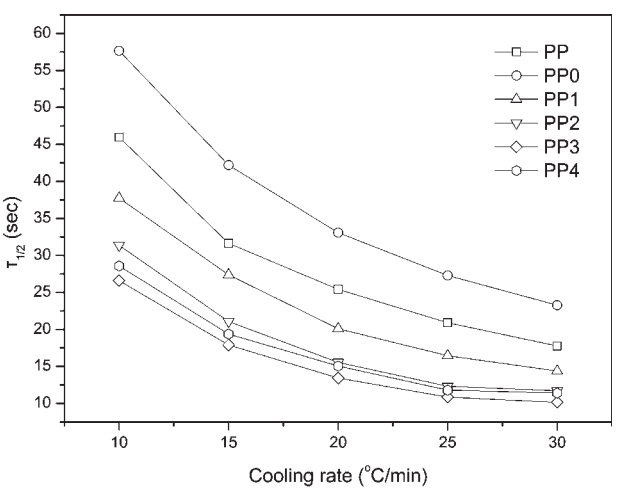

Figure 5 Half-time of crystallization, $\tau_{1/2}$, versus cooling rate for PP and various antibacterial PP composite specimens.

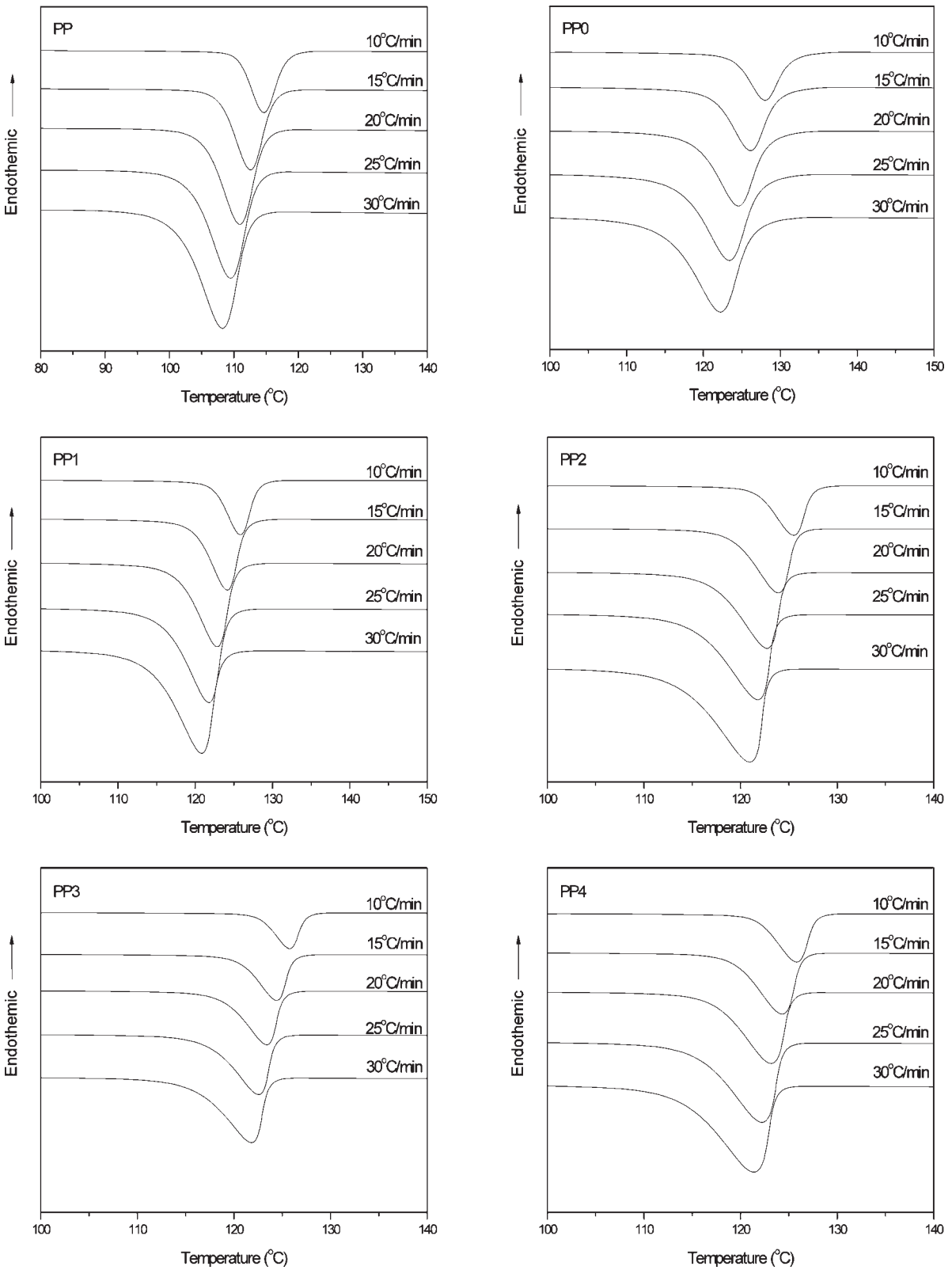

Figure 6 DSC crystallization exotherms of pure PP and antibacterial PP composites crystallized at different cooling rates.

antibacterial PP composite should result from the cooperative interaction between $CaCO_3$, fatty dibasic acid, and PP. As the β-PP content decreases with the increase of cooling rate and antibacterial agent content, it is reasonable to assume that the chain orientation of PP to some extent may be induced by certain microstructure formed by $CaCO_3$ and fatty dibasic acid. Therefore, it is suggested that the formation

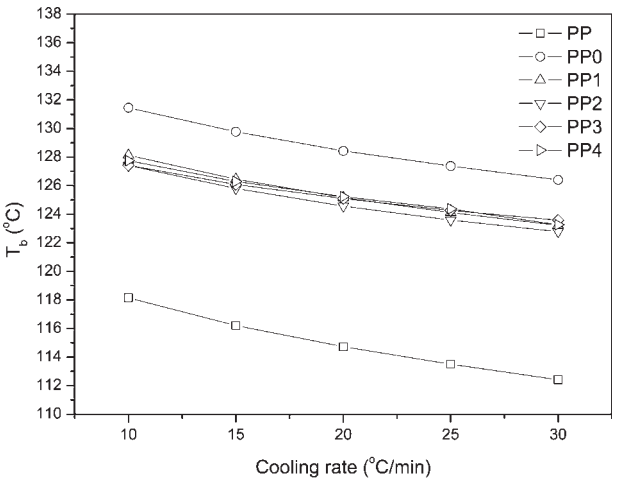

Figure 7 Dependence of crystallization onset temperature (T_o) for pure PP and antibacterial PP composites on cooling rate.

of β-PP here is also orientation induced. Considering that the formation of microstructure by $CaCO_3$ and fatty dibasic acid depends unambiguously on the thermal conditions, the content of β-PP is closely related to the cooling rates given. Furthermore, it is also reasonable to assume that the antibacterial agent to some extent may hinder the formation of certain microstructure between $CaCO_3$ and fatty dibasic acid, thus the content of β-PP is also related to the content of antibacterial agent added.

Crystallization kinetics

It is well known that the half-time of crystallization, $\tau_{1/2}$, is a very important parameter describing the overall crystallization rate. The $\tau_{1/2}$ obtained for pure PP and antibacterial PP composite specimens are plotted against cooling rate in Figure 5. It can be clearly seen from Figure 5 that the $\tau_{1/2}$ of specimen PP0 is higher than that of the other specimens at all cooling rates. The $\tau_{1/2}$ decreases with the increase of antibacterial agent content until 3 phr. The $\tau_{1/2}$ of specimen PP4 with the antibacterial agent content of 4 phr is between that of PP3 and PP2. These results demonstrate that the overall crystallization rate of antibacterial PP composite, which is dependent on the content of antibacterial agent, is faster than pure PP.

Crystallization exotherms of pure PP and antibacterial PP composite at several cooling rates are shown in Figure 6. The nonisothermal crystallization processes of both pure PP and antibacterial PP composite exhibit the same dependence on cooling rate, for example, the crystallization exotherms of antibacterial PP composite shift to lower temperature with the increase of cooling rate. Comparing pure PP with antibacterial PP composite in Figure 6, we can further conclude that the crystallization exotherms of antibacterial PP composite shift to higher temperature with the increase of the antibacterial agent content.

The onset and peak crystallization temperatures (T_o and T_p, respectively) of pure PP and antibacterial PP composites were plotted against cooling rate. As shown in Figure 7, the T_o for antibacterial PP composites is higher than that of pure PP at all cooling rates, indicating the crystallization of antibacterial PP composite starts earlier than that of pure PP. Especially, T_o of PP0 at various cooling rates is considerably high, whereas the difference of onset temperature between other antibacterial PP composite is small. Combined with the results obtained in melting behavior, it is believed that β-nucleating agent was *in situ* formed by $CaCO_3$ and fatty dibasic acid, thereby facilitating the crystallization of antibacterial PP composites. The results are also related to the degree of disperse of antibacterial agent. Similarly, T_p also depends remarkably on the cooling rate and composition of antibacterial PP composite (see Fig. 8). An obvious increase is observed with the decrease of cooling rate and decrease of antibacterial agent content. These changes are consistent with the variation of overall crystallization rate of antibacterial PP composite.

It is clear that the overall crystallization rate increases when compared with pure PP. Furthermore, the overall crystallization rate continuously increases while the β-PP content decreases with the increase of antibacterial agent content. All these show that the crystallization kinetics of antibacterial PP composite with high antibacterial agent content is quite different from that with low antibacterial agent content. This may result from the interactive effect of antibacterial agent and *in situ* formed β-nucleating agent. At low antibacterial agent content, β-nucleat-

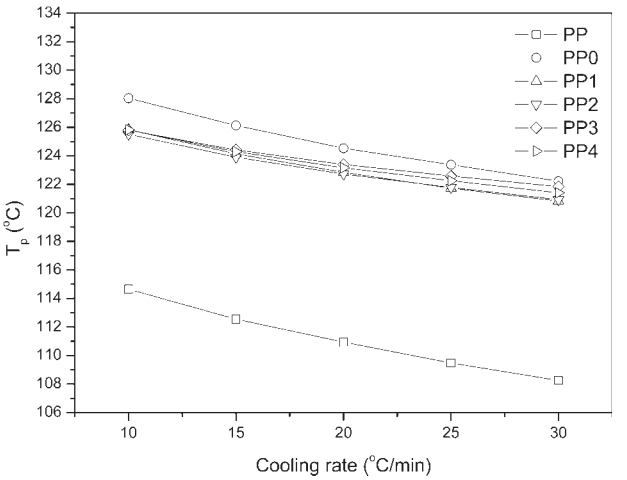

Figure 8 Dependence of crystallization peak temperature (T_p) for pure PP and antibacterial PP composites on cooling rate.

ing agent can be well formed by $CaCO_3$ and fatty dibasic acid, thus facilitating the formation of β-PP crystals. However, this situation was changed at higher antibacterial agent content, extra antibacterial agent may hinder the formation of β-nucleating microstructure, consequently, decrease the content of β-PP crystals formed during crystallization. At the same time, it might decrease the mobility of PP chains in melts, thus making it more difficult for PP to realign into β-modification. On the other hand, extra antibacterial agent took the place of β-nucleating agent as the nuclei and promoted the formation of α-PP in crystallization and the overall crystallinity of antibacterial PP composite.

CONCLUSION

The crystalline morphology and dynamical crystallization behavior of antibacterial PP composite as well as pure polypropylene were investigated. The results reveal that the crystalline structure of antibacterial PP composite changes with the variation of the crystallization conditions and compositions. There exist two crystalline phases, that is, α-modification and β-modification at any given thermal conditions. The formation of β-modification may result from the chain orientation in the melts induced by some microstructure formed by β-nucleating agent. The coexistence of antibacterial agent, β-nucleating agent, results in the increase of overall crystallization rate. On the other hand, the content of β-modification decreases with the increase of antibacterial agent content, and this may be explained in view of the interruptive effect of the antibacterial agent on interaction between components of β-nucleating agent and the obstructing effect on the mobility of PP chains in melts.

References

1. Slawson, R. M.; Van Dyke, M. I.; Lee, H.; Trevors, J. T. Plasmid 1992, 27, 72.
2. Zhao, G. J.; Stevens, S. E. BioMetals 1998, 11, 27.
3. Klueh, U.; Wagner, V.; Kelly, S.; Johnson, A.; Bryers, J. D. J Biomed Mater Res 2000, 53, 621.
4. Russel, A. D.; Chopra, I.; Hemel, H. H. Understanding Antibacterial Action and Resistance; Ellis Horwood: Chichester, England, 1996; Chapter 3.
5. Spadaro, J. A.; Chase, S. E.; Webster, D. A. J Biomed Mater Res 1986, 20, 565.
6. Feng, G. L.; Wu, J.; Chen, G. Q.; Cui, F. Z.; Kim, T. M.; Kim, J. O. J Biomed Mater Res 2000, 52, 662.
7. Spardo, J. A.; Berger, T. J.; Barranco, S. D.; Chapin, S. E.; Becker, R. O. Microb Agents Chemother 1974, 6, 637.
8. Wohrmann, R. M. J.; Hentschel, T.; Munstedt, H. Adv Eng Mater 2000, 2, 380.
9. Kumar, R.; Munstedt, H. Biomaterials 2005, 26, 2081.
10. Turner-Jones, A.; Aizlewood, J. M.; Beckett, D. R. Makromol Chem 1964, 75, 134.
11. Jacoby, P.; Bersted, B. H.; Kissel, W. J.; Smith, C. E. J Polym Sci Polym Phys 1986, 24, 461.
12. Aboulfaraj, M.; G'sell, C.; Ulrich, B.; Dahoun, A. Polymer 1995, 36, 731.
13. Karger-Kocsis, J.; Varga, J. J Appl Polym Sci 1996, 62, 291.
14. Tjong, S. C.; Shen, J. S.; Li, R. K. Y. Polym Eng Sci 1996, 36, 100.
15. Tjong, S. C.; Shen, J. S.; Li, R. K. Y. Polymer 1996, 37, 2309.
16. Mubarak, Y.; Harkin-Jones, E. M. A.; Martin, P. J.; Ahmad, M. Polymer 2001, 42, 3171.
17. Li, J. X.; Cheung, W. L.; Jia, D. M. Polymer 1999, 40, 1219.
18. Li, J. X.; Cheung, W. L. Polymer 1998, 39, 6935.
19. Padden, F. J.; Keith, H. D. J Appl Phys 1959, 30, 1479.
20. Padden, F. J.; Keith, H. D. J Appl Phys 1966, 37, 4013.
21. Padden, F. J.; Keith, H. D. J Appl Phys 1973, 44, 1217.
22. Samuels, R. J.; Yee, R. Y. J Polym Sci Part A-2: Polym Phys 1972, 10, 385.
23. Turner-Jones, A.; Aizlewood, J.; Beckett, D. Makromol Chem 1964, 75, 134.
24. Guerra, G.; Petracone, V.; Corradini, P.; De-Rossa, C.; Napolitano, R.; Pirozzi, B. J Polym Sci: Polym Phys Ed 1984, 22, 1029.
25. Petracone, V.; Guerra, G.; De-Rossa, C.; Tuzu, A. Macromolecules 1985, 18, 813.
26. Petracone, V.; De-Rossa, C.; Guerra, G.; Tuzu, A. Macromol Chem Rapid Commun 1984, 5, 631.
27. Janimak, J. J.; Cheng, S. Z. D.; Zhang, A.; Hsieh, E. T. Polymer 1992, 33, 728.
28. Grein, C.; Plummer, C. J. G.; Kausch, H. H.; Germain, Y.; Beguelin, Ph. Polymer 2002, 43, 3279.
29. Turner-Jones, A.; Cobbold, A. J J Polym Sci 1968, 6, 539.
30. Norton, D. R.; Keller, A. Polymer 1985, 26, 704.
31. Lovinger, A. J.; Chua, J. O.; Gryte, C. C. J Polym Sci: Polym Phys Ed 1977, 15, 641.
32. Garbarczyk, J.; Paukzta, D. Polymer 1981, 22, 562.
33. Lotz, B.; Fillon, B.; Therry, A.; Wittmann, J. C. Polym Bull 1991, 25, 101.
34. Varga, J. J Thermal Anal 1989, 35, 1891.
35. Varga, J. J Mater Sci 1992, 27, 2557.
36. Varga, J.; Karger-Kocsis, J. Polym Bull 1993, 30, 105.
37. Varga, J.; Karger-Kocsis, J. Polymer 1995, 36, 4877.
38. Varga, J.; Karger-Kocsis, J. J Mater Sci Lett 1994, 13, 1069.
39. Varga, J.; Karger-Kocsis, J. J Polym Sci Part B: Polym Phys 1996, 34, 657.
40. Li, H.; Jiang, S.; Wang, J.; Wang, D; Yan, S. Macromolecules 2003, 36, 2802.
41. Li, H.; Zhang, X.; Kuang, X.; Wang, J.; Wang, D.; Li, L.; Yan, S. Macromolecules 2004, 37, 2847.